Anal Bioanal Chem (2005) 383: 576–586
DOI 10.1007/s00216-005-0028-3

ORIGINAL PAPER

Jiří Petřek · Jan Víteček · Helena Vlašínová · René Kizek · Karl J. Kramer · Vojtěch Adam · Bořivoj Klejdus · Ladislav Havel

Application of computer imaging, stripping voltammetry and mass spectrometry to study the effect of lead (Pb-EDTA) on the growth and viability of early somatic embryos of Norway spruce (*Picea abies* /L./ Karst.)

Received: 10 January 2005 / Revised: 8 July 2005 / Accepted: 13 July 2005 / Published online: 12 October 2005

Abstract Image analysis (IA) was used to determine the areas and circumferences of clusters of early somatic embryos (ESEs) of the Norway spruce (*Picea abies* /L./Karst.). Results obtained from IA were compared with the fresh weights of the ESE clusters and their esterase activities. The areas of the ESE clusters correlated well with both the increases in fresh weight (R^2=0.99) of the ESEs and their esterase activities (R^2=0.99). In addition, we studied the viability of the ESEs, which was determined by (a) double staining with fluorescein diacetate and propidium iodide (the resulting fluorescence was quantified by IA) and (b) determining esterase activity using a spectrofluorimetric detector. The results obtained with IA and esterase assay were comparable (the deviation between the tangents of the bisectors was 6.4%). IA was also used to study the effect of Pb–EDTA chelate (50, 250 and 500 μM) on the viability of the ESEs and on the growth of clusters. The presence of Pb–EDTA markedly slowed the growth of ESEs clusters (by more than 65% with 250 μM of Pb–EDTA after 288 h of cultivation) and decreased the viability of ESEs (by more than 30% with 500 μM of Pb–EDTA after 288 h of cultivation). The lead concentration in the ESEs was determined by differential pulse anodic stripping voltammetry and increased with the external lead concentration and the time of treatment from 100 to 600 pg Pb/100 mg of fresh weight of ESEs. Glutathione is a diagnostic marker of the influence of Pb–EDTA on ESEs and its content was determined by high–performance liquid chromatography coupled with mass spectrometry. The glutathione content changed linearly with treatment time and the applied external lead concentration. The highest glutathione content was obtained at 250 μM of Pb–EDTA after 192 h of cultivation.

Keywords Early somatic embryo of Spruce · Computer image analysis · Lead · Glutathione · Differential pulse anodic stripping voltammetry

Abbreviations *IA*: computer image analysis · *ESE*: early somatic embryo · *CCD*: charge-coupled device · *Pb-EDTA*: lead (II)-ethylene diamine tetra-acetic acid · *FDA*: fluorescein diacetate · *PI*: propidium iodide · *GSH*: glutathione · *HPLC-MS*: High-performance liquid chromatography mass spectrometry · *DPASV*: Differential pulse anodic stripping voltammetry

J. Petřek · J. Víteček · H. Vlašínová · L. Havel
Department of Botany and Plant Physiology,
Mendel University of Agriculture and Forestry,
Zemědělská 1, 613 00,
Brno, Czech Republic

R. Kizek (✉) · V. Adam · B. Klejdus
Department of Chemistry and Biochemistry,
Mendel University of Agriculture and Forestry,
Zemědělská 1, 613 00,
Brno, Czech Republic
e-mail: kizek@sci.muni.cz
Tel.: +420-5-45133350
Fax: +420-5-45212044

K. J. Kramer
Grain Marketing and Production Research Center
Agricultural Research Service,
US Department of Agriculture,
Manhattan, KS 66502, USA

V. Adam
Department of Analytical Chemistry,
Faculty of Science,
Kotlarska 2, 611 37,
Brno, Czech Republic

Introduction

The plant growth curve is a fundamental parameter for a plant physiologist and its measurement in plant tissues and cell cultures can be accomplished using several different methods [1]. The most frequently used methods are based on the counting and/or weighing of cells or tissues [1]. The disadvantages of these methods are the destruction and/or contamination of cultures during analysis. In recent years,

image analysis (IA) has been used as a tool to study the growth and/or morphology in prokaryotic and/or eukaryotic cell cultures [2–5]. IA has been used to study culture growth and morphology (cell density, shape, size or color) and somatic embryogenesis, for example in *Daucus carota* [4, 6, 7], *Betula pendula* [8], *Ipomoea batatas* [9], *Saccharum* spp. [10] and *Picea abies* [11]. The theoretical aspects of related computer image analysis have been summarized in several publications [6–8].

Pollutants containing heavy metals and toxic organic substances often enter the ecosystem due to the application of fertilizers, pesticides and other industrial products [12–15]. Studies of plant responses to heavy metal stress are especially important to our understanding of a number of biological processes [11, 16–18] because the presence of heavy metals in the plant cell activates protective mechanisms. They initiate the synthesis of cysteine-containing compounds (such as glutathione) used in detoxification processes [11, 18–21]. A number of analytical techniques have been developed to determine plant biological active compounds [17, 22–28].

In our work we used image analysis to determine the areas and circumferences of clusters of early somatic embryos (ESEs) of the Norway spruce. The viability of the ESEs was determined by (a) double staining with fluorescein diacetate (FDA) and propidium iodide (PI), which was quantified by IA and (b) esterase activity, which was determined using a spectrofluorimetric detector. We recently published papers where we discussed the advantages of the esterase assay as a suitable marker for the determination of basic growth parameters of plant cell cultures [29, 30]. IA was also applied to study the effects of Pb–EDTA chelate (50, 250 and 500 μM) on the viability of ESEs and on the growth of their clusters. Although the influence of lead on organisms has been studied for many years, its biochemical mechanism of action is still unclear. Moreover, it is interesting that lead creates characteristic morphologic formations in plant cell tissues [31]. Based on these reasons, we studied the influence of lead on the ESEs. Glutathione and lead concentrations in the ESEs were determined by high-performance liquid chromatography coupled with mass spectrometry (HPLC–MS) and differential pulse anodic stripping voltammetry (DPASV), respectively.

Materials and methods

Plant material

ESE clones of the Norway spruce (*Picea abies* /L./ Karst.) designated as 2/32, E2, 3/5H, and blue spruce (*Picea pungens* Engelm.) designated as PE 14 were used in our experiments. The clones were originally established at the Department of Botany and Plant Physiology of the Mendel University of Agriculture and Forestry in Brno, Czech Republic, according to the procedures described in [32, 33].

Cultivation conditions

The cultures were maintained on a semisolid (Gelrite Gellan Gum, Merck, Germany) half-strength LP medium [34] with modifications [35]. The concentrations of 2,4-dichlorofenoxyacetic acid and N^6-benzyladenine were 4.4 and 9 μM, respectively. The pH value was adjusted to 5.7–5.8 before autoclaving (121°C, 100 kPa, 20 min). The organic part of the medium, excluding saccharose, was sterilized by filtration through a 0.2 μm polyethylenesulfone membrane (Whatman, Puradisc 25 AS). Ten ESE clusters were cultivated in one plastic Petri dish (100 mm in diameter) containing 30 ml of the medium. Subcultivation of stock cultures was performed at two-week intervals. The stock and experimental cultures were maintained in a cultivation box in the dark at a temperature of 23±2°C.

Pb-EDTA LP modified medium

The ESE clusters of clone 2/32 were cultivated on a modified LP medium with lead chelate (Pb-EDTA) added in concentrations of 50, 250 and 500 μM. A stock solution of Pb-EDTA was prepared [36] by mixing $Pb(NO_3)_2$ with ethylene diamine tetra-acetic acid (EDTA) in a 1:1 molar ratio and stirred at 50°C for 1 h. The filter-sterilized Pb-EDTA complex was added to the autoclaved culture medium.

Detection procedures

Weight analysis

The growth of ESEs clusters was quantified by weighing (APX–153, Denver Instrument, Göttingen, Germany). The semisolid medium was carefully cleared away (washed in 0.2 M phosphate buffer, pH 7.0) from the ESE clusters before weighing and the fresh weights of single ESE clusters were determined as quickly as possible to avoid desiccation.

Computer image analysis

To obtain grayscale images, a charge-coupled device camera (UVP–GDS 8000 CCD, Sony, Tokyo, Japan) connected to a personal computer was used. The CCD camera had a flexible head and could take images of ESE clusters through the lid of a Petri dish. The images were recorded at the beginning of the cultivation and at certain intervals until the end of the cultivation. The data were converted to digital images using the Grab-IT (version 1.3) program. The areas and circumferences of the ESE clusters in the digital images were calculated using the program Image-Pro Plus, (Sony, ver. 1.3). The data were processed in Excel (Microsoft, Redmond, WA). The experimental design of IA is shown in Fig. 1A.

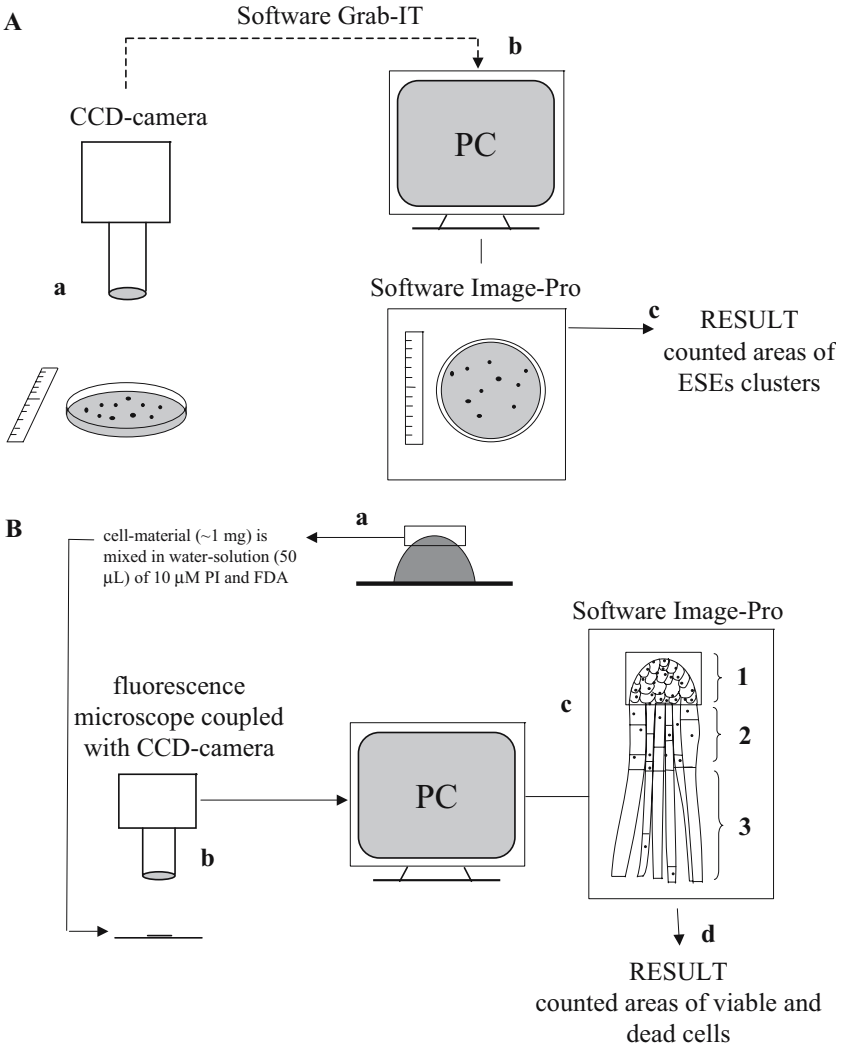

Fig. 1A–B Scheme of the experimental design used for computer image analysis. **A** Determination of areas and circumferences of ESE clusters. (a) Petri dish with ESE clusters is transferred to the stand of the CCD camera with scale. (b) The data acquired with the CCD camera are converted into digital images using the program Grab-IT. (c) The areas and circumferences of the ESE clusters are calculated from the digital image by Image-Pro software. **B** Determining the viability of the ESEs. (a) ESE clusters (~1 mg) used for viability determination of ESEs are prepared from the upper part of the cluster. Cell material is mixed with fluorescein diacetate (FDA) and propidium iodide (PI) and after 5 min the images are taken using the (b) fluorescent microscope coupled to a CCD camera. (c) Acquired digital images are processed using Image-Pro software. Percentages of green and red areas in the compact embryonic group of ESEs (marked by frame) were used to measure the viable and dead cells, respectively. Scheme of ESE: (1) compact embryonic group, (2) embryonic tubes, (3) suspensor cells. For other details, see "Materials and methods" section

Esterase assay

Samples of ESE clusters (100–200 mg fresh weight) were washed in buffer (50 mM potassium phosphate, pH 8.7) and centrifuged at 360×*g*; 10 min; 20°C (centrifuge MR 22 by Jouan, Winchester, VA). This step was repeated twice. The resultant pellet was kept at –20°C until receipt. Thawed samples were diluted to a volume of 1 ml with extraction buffer (250 mM potassium phosphate, 1 mM DTT, pH 8.7) and disintegrated (10 min) using a Potter–Elvehjem homogenizer placed in an ice bath. The homogenate was centrifuged at 10,000×*g*; 15 min; 4°C (centrifuge MR 22 by Jouan). An aliquot (5 µl) of supernatant was mixed with 985 µl of 1 M phosphate buffer (pH 8.7) and the reaction was started by the addition of 10 µl of 500 µM FDA solution in anhydrous acetone. The amount of acetone in the reaction mixture was 1% (v/v). After incubation (15 min, 45°C), an aliquot of the reaction mixture (10 µl) was diluted with 1990 µl of 250 mM phosphate buffer (pH 8.7). The fluorescence of fluorescein ($\lambda_{excitation}$=490 nm and $\lambda_{emission}$=514 nm) was read immediately using a spectrofluorimetric detector (RF–551 by Shimadzu, Kyoto, Japan) [30]. Esterase activity in international units (IU, one unit liberates one µmol of fluorescein per minute under specified conditions, 45°C) was recalculated to relative units.

Double staining

Modified double staining with FDA and propidium iodide was used to determine the viability of the ESEs [37]. FDA causes green fluorescence in viable cells because the nonfluorescent FDA easily penetrates into viable cells where it is hydrolyzed to the brightly fluorescent fluorescein ($\lambda_{excitation}$=490 nm and $\lambda_{emission}$=514 nm) which does not readily diffuse out through the cytoplasmatic membrane. The red fluorescence of PI ($\lambda_{excitation}$=536 nm and $\lambda_{emission}$=620 nm) in cells shows that these cells are dead because this compound cannot pass through the functional cytoplasmatic membrane. In our experiments the ESEs (~1 mg) were harvested and diluted with water to a final volume of 50 µl. Stock solutions of PI and FDA were added to a final concentration of 20 µg ml^{-1} and 1 µg ml^{-1},

respectively. After 5 min of incubation at room temperature, the percentage of dead (red-stained cells) and viable cells (green-stained cells) was evaluated using an Olympus AX 70 fluorescence microscope with an Olympus cube U–MWU linked to the Olympus digital camera (4040 Zoom). In addition, areas of dead cells (red staining) and viable cells (green staining) were marked using the Image-Pro program and the sizes of the stained areas were determined. The percentage of red (dead cells) and green areas (viable cells), respectively, in each digital image was measured (see Fig. 1B).

Lead determination

Recently we developed an electrochemical method for the detection of Pb in plant material [16]. Samples (ESEs) were washed with 1 M EDTA in 0.2 M phosphate buffer (pH 7.0) to remove their cultivation media, and centrifuged for 5 min at 3000×*g* (Eppendorf 5402, New York, USA). Then they were transferred to a test tube and frozen by immersion in liquid nitrogen to disrupt the ESE. The extract was then added to 1 ml of 0.2 M phosphate buffer (pH 7.0), homogenized by vortexing for 15 min (Vortex–2 Genie, Scientific Industries, New York, USA), and finally sonicated for 5 min at 200 W (Bandelin, Berlin, Germany). The homogenate was then centrifuged at 14,000×*g*, 30 min at 4°C (Eppendorf 5402). The supernatant (1 ml) was mixed with HCl (35%) for 30 min. After mixing, the deproteinized solution was neutralized by 13 M NaOH and added to 1 ml of supporting electrolyte (0.1 M phosphate buffer, pH 5.5). The solution was deoxygenated for 2 min by purging with water-saturated argon (99.999%) prior to measurements. Differential pulse anodic stripping voltammetry (DPASV) was used for the determination of lead. Electrochemical measurements were carried out using an AUTOLAB electrochemical instrument (EcoChemie, Utrecht, Netherlands) connected to a VA Stand 663 (Metrohm, Herisau, Switzerland). A three-electrode system was used, consisting of a hanging mercury drop electrode (HMDE) as a working electrode with an area of 0.4 mm^2, an Ag/AgCl/3 mol l^{-1} KCl as a reference electrode and a Pt wire as an auxiliary electrode [38]. GPES software (EcoChemie) was utilized for the treatment of raw data, using level 4 of the Savitzky–Golay filter [39]. Pb was deposited on the HMDE at a potential of –0.6 V for 60 s. During deposition the processing solution was stirred (1450 rpm). The anodic scan was initialized at –0.6 V and stopped at 0 V. The step potential was 5 mV, modulation amplitude 50 mV, and time interval 0.24 s. Other experimental details are described in [16].

HPLC–MS determination of GSH

ESEs were washed with 1 M EDTA in 0.2 M phosphate buffer (pH 7.0) and centrifuged for 5 min at 3,000×*g* (Eppendorf 5402). ESEs (about 20 mg) rinsed of their cultivation media were frozen three times in liquid nitrogen to disrupt the cells and then transferred to a test tube with a 500 µl solution containing 1 mM dithiothreitol and 30 mM ascorbic acid. The frozen samples were homogenized by shaking in a Vortex–2 Genie for 5 min at 4°C (Scientific Industries) and sonicated using a Bandelin Sonopuls HD 2070 for 10 s at 7 W. The homogenate was centrifuged (14,000×*g*) for 15 min at 4°C using a Universal 32 R centrifuge (Hettich–Zentrifugen, Germany). The supernatant was filtered through a membrane filter (0.45 µm, Millipore, Bedford, MA, USA) before its injection into a chromatographic column.

An HP 1100 chromatographic system (Hewlett–Packard, Waldbronn, Germany) was equipped with a vacuum degasser (G1322A), a binary pump (G1312A), an autosampler (G13113A), a column thermostat (G1316A) and a diode array detector (model G1315A). The system was coupled on-line to a mass-selective HP MSD detector (G 1946A, Hewlett-Packard, Palo Alto, CA, USA). GSH was separated using an Atlantis HILIC Silica chromatographic column (3 µm particle size; 2.1×150 mm) in an isocratic mode with acetonitrile and trifluoroacetic acid. The flow rate was 0.15 ml min^{-1}. The temperature of the column oven was set at 20°C. The column effluent was monitored with a diode array detector and directly introduced into the quadruple mass spectrometer operated in positive ESI mode. The mass spectrometer was regularly calibrated with an ESI tuning solution obtained from Hewlett-Packard. The nebulizer gas pressure was 350 kPa, the drying gas was nitrogen at 10 l min^{-1}at a temperature of 350°C, the capillary voltage was 4000 V, and the gain was 1. The *m/z* spectra and data for the selected ion-monitoring (SIM) mode were recorded for glutathione (molecular weight of GSH is 307 (M); *m/z* 308 corresponds to $[M+H]^+$; *m/z* 330 to $[M+Na]^+$; *m/z* 179 and *m/z* 233 peaks to fragmentation of GSH). Thiosalylcilic acid (TSA) was used as an internal standard for the glutathione determination [40].

Statistical analysis

STATGRAPHICS software (Statistical Graphics Corp, Englewood Cliffs, NJ, USA) was used for statistical analyses. Results are expressed as the means ± S.D. unless noted otherwise. A value of $p<0.05$ was considered significant.

Results and discussion

The growth curve and the percentage of viable and dead cells (viability) are basic parameters for studying the influence of abiotic and biotic stresses on early somatic embryos (ESEs), which can be characterized using various methods such as weight analysis, double staining and esterase assay [1, 30]. As we mentioned in the "Introduction", all of the methods mentioned here are laborious and/or destructive. A nondestructive IA could simplify the determination of these culture characteristics. That is why we studied the correlation between IA and the older methods mentioned here. For this purpose we used the Norway spruce early somatic embryo clone 2/32 as a model system.

Growth analysis

During the cultivation of ESE clone 2/32, the cells of the embryonic group (Fig. 2A, (a)) divide continuously and new tubular (Fig. 2A, (b)) and suspensor (Fig. 2A, (c)) cells are formed at the distal part of the embryo [41, 42]. ESEs form a cluster of cells (Fig. 2B) on the surface of a semisolid medium. In our experiments we cultivated ten ESEs clusters in a plastic Petri dish (Fig. 2C) for 14 days.

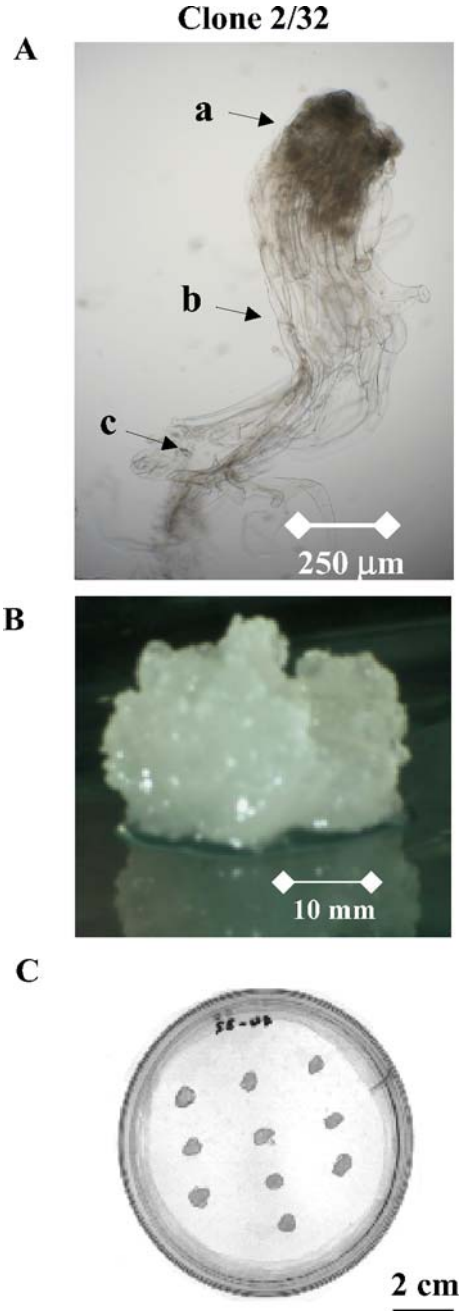

Fig. 2A–C Early somatic embryos of the Norway spruce of clone 2/32 after 14 days of cultivation on modified LP medium in the dark at 23±2°C. **A** Photography of an early somatic embryo: (a) embryonic group, (b) embryonic tubes, (c) embryonic suspensor. **B** Cluster of early somatic embryos. **C** Petri dish with clusters of early somatic embryos

Weight analysis

A simple technique for estimating a growth curve is to determine the change in fresh weight as a function of cultivation time. The resulting growth curve of the ESEs is shown in Fig. 3A. From the results obtained it follows that the increase in fresh weight is linear with cultivation time for the first 14 days after subcultivation (y=14.58x–6.94; R^2=0.99; see Fig. 3A). On the other hand, manual weighing of the clusters has some disadvantages (such as stress, contamination, desiccation, clusters must be washed free from the adhering medium). Desiccation is rapid (after 30 minutes there was more than 40% fresh weight loss; upper inset in Fig. 3A). The desiccation and denuding medium are obstacles for routine work.

Computer image analysis

Image analysis (IA) has been already shown to be a good tool for determining the sizes and shapes of structures like cells and somatic embryos [3, 6–8, 43] and it could provide an alternative approach to weight analysis. Analytical images of ESE clusters were recorded from a closed Petri dish through its lid to allow studies of the same clusters during the whole cultivation period without stress. 8-bit grayscale ESEs cluster images with resolutions of 5 pixels/mm^2 were found to be optimal (data not shown). When we recorded the area of one ESE cluster of clone 2/32 ten times by IA under these conditions, we found that the biggest difference in single values gave a relative standard deviation of only 0.31%. Noting the increases in the areas of ten different ESEs clusters (which had approximately the same starting areas and circumferences) in the same Petri dish, we found that the biggest difference between the increases in the areas of single clusters was 12–16%. The resulting growth curve (dependence of increase of ESE cluster area on cultivation time) is shown in Fig. 3B. From the results obtained it follows that the ESE cluster area increases with cultivation time in a linear fashion for the first 14 days after subcultivation (y=12.39x–4.21, R^2=0.99; see Fig. 3B). In the case of desiccation, we did not observe any changes in ESE cluster areas during IA analysis (bottom inset in Fig. 3B).

Esterase assay

Recently we observed that esterase activity can be used as a growth marker for ESEs [30]. The resulting growth curve is shown in Fig. 3C. From the results obtained it follows that esterase activity increases with cultivation time in a linear manner for the first 14 days after subcultivation (y=14.45x–7.53; R^2=0.99; see Fig. 3C). A disadvantage of esterase assays is the destruction of the ESE clusters observed.

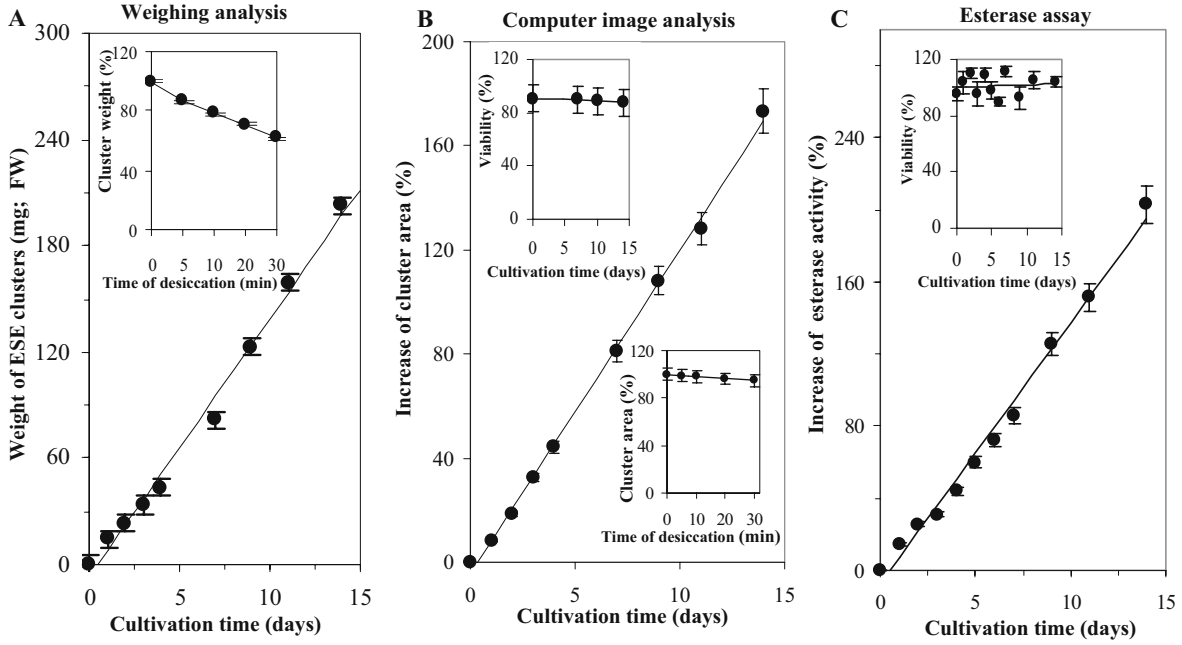

Fig. 3A–C Estimation of growth curve of ESE clone 2/32 clusters during 14 days of cultivation on modified LP medium in the dark at 23±2°C by (**A**) weight analysis; *inset*, dependence of cluster weight on time of desiccation, (**B**) computer image analysis; *upper inset*, dependence of viability of ESEs on cultivation time, which was detected by IA coupled with fluorescence microscope, and *bottom inset*, dependence of cluster area on time of desiccation, and (**C**) esterase assay; *inset*, dependence of viability of ESEs on cultivation time. An ESE cluster area of 14 mm^2 and esterase activity of 0.0026 IU was taken as 100%. Values represent an average of ten ESE clusters

Comparison of IA with weight analysis and esterase assay

Results obtained from IA were compared with weight analysis and esterase assay results. The dependence of the increase of ESE cluster area on (a) its fresh weight and (b) esterase activity is shown in Fig. 4A,B. From the results obtained, it follows that both relationships are linear (for fresh weight y=0.61x–0.39; R^2=0.99, Fig. 4A; for esterase activity y=0.62x+0.21; R^2=0.99, Fig. 4B). The linear

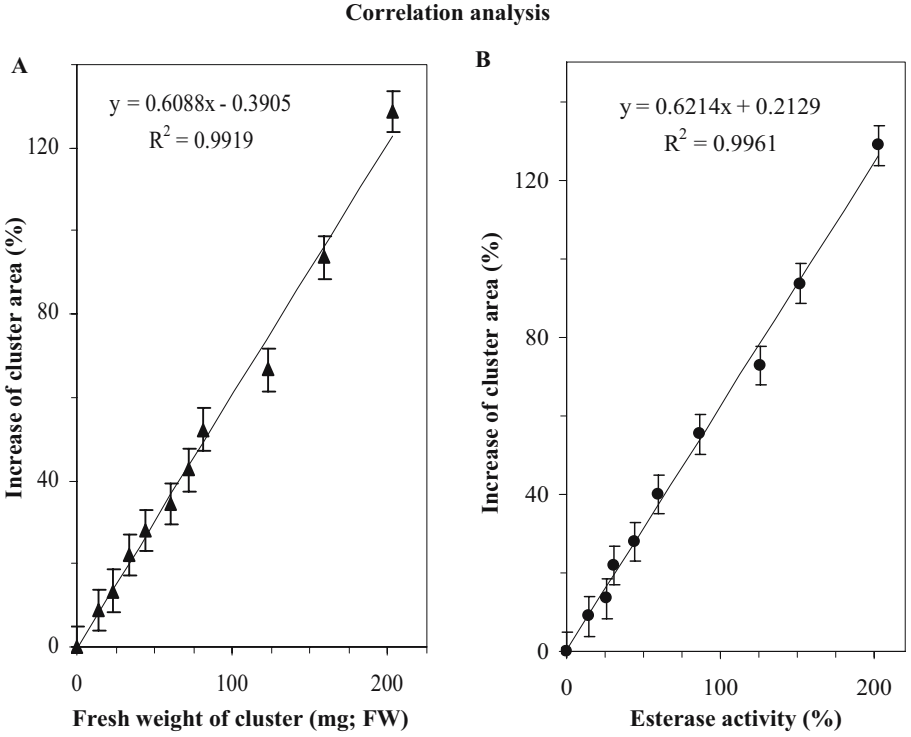

Fig. 4A–B Correlation analysis of cluster area. Dependence of increase in ESE cluster area on (**A**) the cluster's fresh weight and (**B**) its ESE esterase activity. Other details are described in Fig. 3

correlation between area size and fresh weight occurred until the end of second week of cultivation, when the fresh weight increased faster than the area. These observations suggest that the ESEs clusters grow equally as quickly in all directions at the beginning of the cultivation for about two weeks and then they do not grow equally in all directions.

Viability of ESEs

Procedures for estimating cell viability are usually based on dye exclusion tests and/or measurement of enzyme activities. In our experiments we determined the viability of ESEs by (a) double staining with fluorescein diacetate and propidium iodide (the resulting fluorescence was quantified by IA), and (b) esterase activity, which was determined using a spectrofluorimetric detector.

Computer image analysis

A modified method for double staining with fluorescein diacetate (FDA) and propidium iodide (PI) in order to determine the viability of ESEs was used, as described in [37, 44]. For our purposes, only the fluorescent areas of embryonic groups of ESEs were taken into account because the embryonic tube and suspensor cells are dying or dead as a result of the developmental patterns of ESEs [35, 42]. When we observed ESE cells under a fluorescent microscope after the application of FDA and PI, we found that it was difficult to count the cells because the ESE cells were superimposed in several layers. We assumed that IA could solve this problem. The ESE cells that fluoresce according to their viability were quantified using IA coupled to a fluorescence microscope. The linear dependence of viability (as determined by IA of the fluorescence) on cultivation time for the first 14 days after subcultivation is shown in the upper inset in Fig. 3B.

Esterase activity

We also used intracellular esterase activity determination, which was previously shown to be applicable to a viability assay [30]. We observed that the intracellular esterase activity of a constant amount of ESEs did not change significantly during the period of the experiment (inset in Fig. 3C). The intracellular esterase activity of ESEs was proportional to its viability and was negligible in the dead embryonic mass that was obtained by heating (65°C) ESEs for 30 min (not shown).

Comparison of IA with esterase assay

Results obtained using IA on FDA/PI stained cells were compared with esterase assay results, and these correlated well (deviation between the tangents of the bisectors was only 6.4%). The results suggest that IA can be used for viability determinations of ESEs.

Study of ESE clusters using IA

Size and form of ESE cluster

During our experiments we observed that the increase in area of the ESE clusters probably depended on their size at the beginning of subcultivation. That is why we tested the influence of the initial area of the ESE cluster of clone 2/32 [the area size of clusters at the beginning of the experiment was (see X axis): (1) 3 mm^2, (2) 6.7 mm^2, (3) 14.2 mm^2, (4) 29.4 mm^2, (5) 62.9 mm^2] on the increase in area. The biggest increase in area was obtained for a starting area of 6.7 mm^2 (Fig. 5). The optimal starting area resulted in the largest increase in growth, whereas smaller or larger sizes of ESE clusters showed smaller increases in size (maximal decrease was about 30%, see Fig. 5).

In addition, we prepared five different forms of ESE clone 2/32 clusters (A, B, C, D, E; see Fig. 6A) during the subcultivation process and measured their circumferences and area sizes by IA over a 14 day-long cultivation period. Using the ratio of *a* to *b* (two perpendicular diameters that represent the longest perpendicular axes of the cluster, see Fig. 6A), we defined two kinds of experimental cluster shapes: rounded (ratio>0.8; clusters A, B and C) and

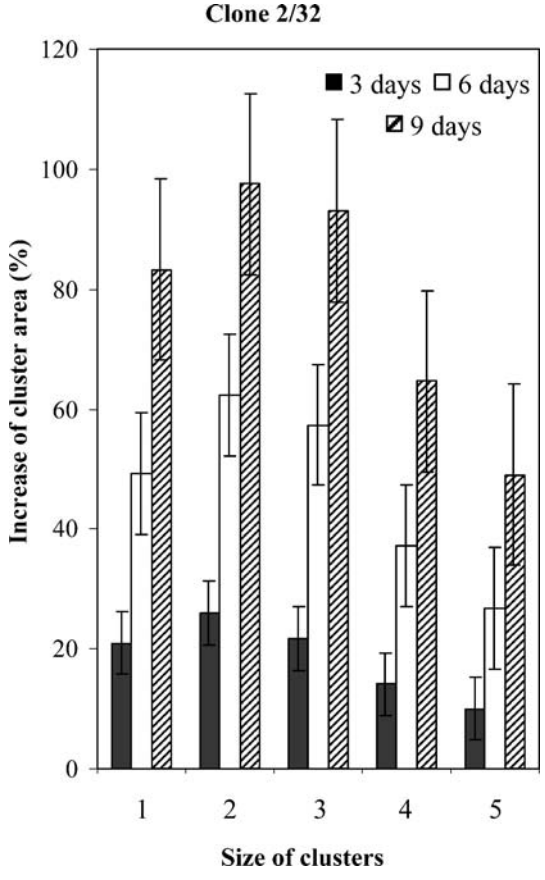

Fig. 5 The effect of area of ESE cluster of clone 2/32 at the beginning of the experiment (see X axis): (**1**) 3 mm^2, (**2**) 6.7 mm^2, (**3**) 14.2 mm^2, (**4**) 29.4 mm^2, (**5**) 62.9 mm^2) on the growth after 3 (*black columns*), 6 (*unfilled columns*) and 9 days (*striped columns*) of cultivation. Other experimental details are given in Fig. 3

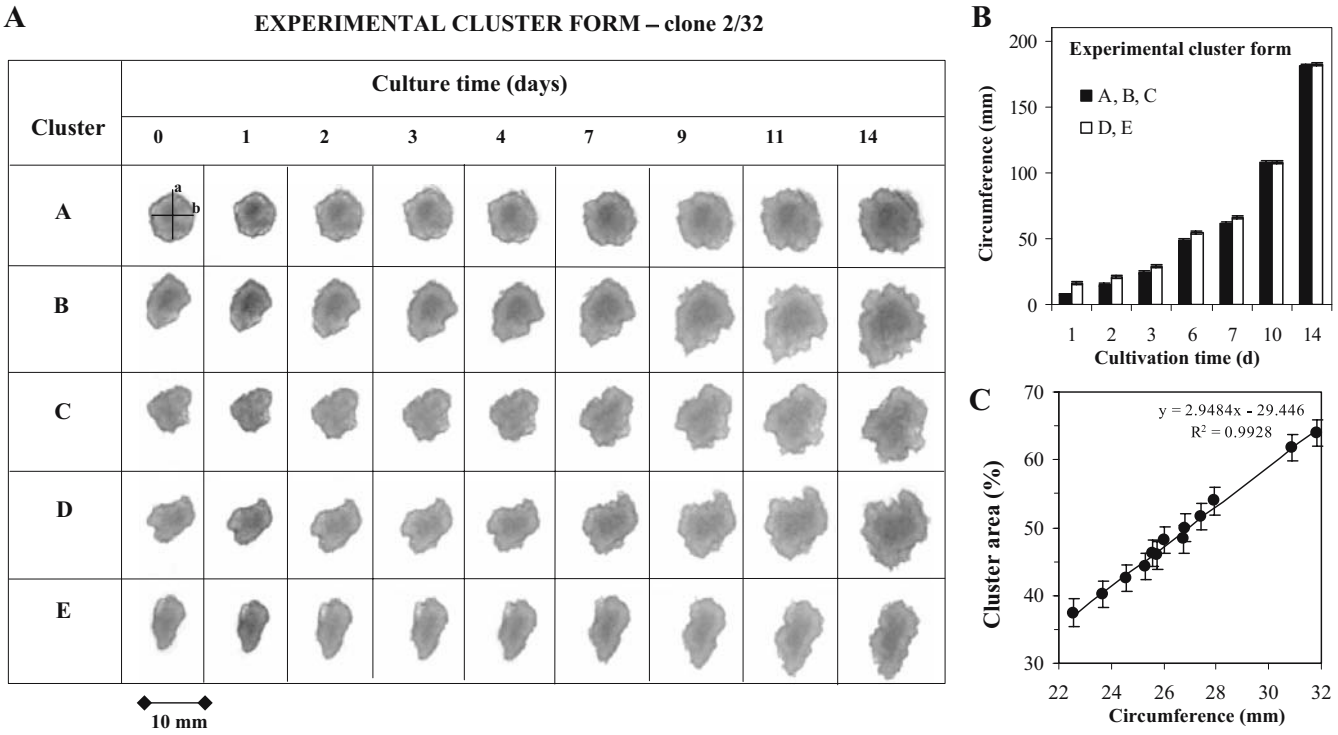

Fig. 6A–C **A** Different shapes of clusters [using the ratio of *a* to *b* (two perpendicular diameters which represent the longest perpendicular axes of the cluster, see Fig. 6)]. We defined two experimental cluster shapes: rounded (the ratio>0.8; clusters A, B and C) and elongated (the ratio<0.8; clusters D and E). **B** Dependence of ESE cluster circumference on the cultivation times of different cluster shapes. **C** Correlation between cluster area and cluster circumference. Other experimental details are given in the legend of Fig. 5

elongated (ratio<0.8; clusters D and E) (Fig. 6A). When we compared the circumferences of ESE clusters with rounded and elongated shapes, we found that many elongated clusters became more rounded (Fig. 6A,B). Furthermore, we cultivated clusters with approximately the same fresh weight and area but different circumferences at the beginning of the experiment to investigate the influence of the circumference on growth (Fig. 6C). The clusters with a longer circumference at the beginning of the experiment had a greater fresh weights and areas at the end of the experiment than clusters that had shorter initial circumferences (Fig. 6C). The influence of the circumference on growth is probably related to the influence of circumference on the uptake of nutrition from the medium. The same influence of the circumference was also observed by [32] when they studied different ESE genotypes of the Norway spruce.

ESE genotypes

The genotype of the ESE plays an important role in the formation and growth of its cluster. That is why, in addition to clone 2/32 of the Norway spruce, we also studied clones E2 and 3/5H of the same species and clone PE14 of the blue spruce, whose cluster forms are different (Fig. 7A). The IA results showed that these other clones had a similar growth curve to clone 2/32 (Fig. 7B).

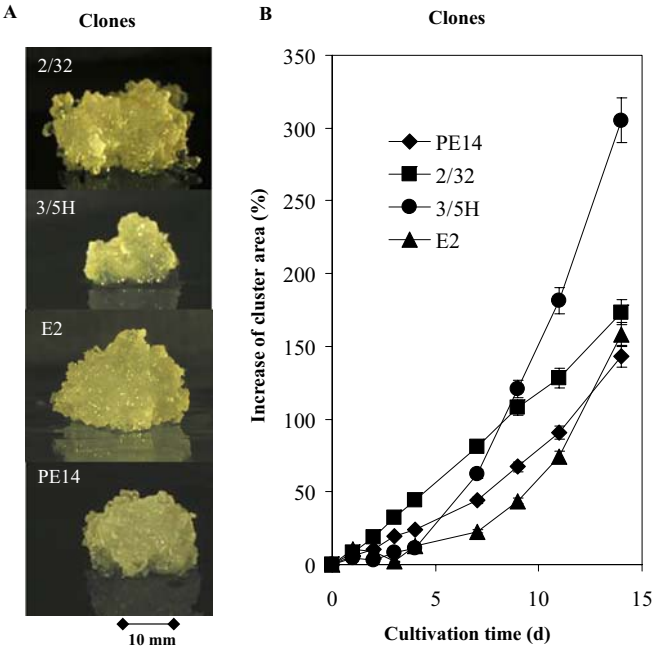

Fig. 7A–B Study of ESE clusters of clones 2/32, E2 and 3/5H of the Norway spruce and clone PE14 of blue spruce. **A** Photograph of typical single ESE clusters of different clones. **B** The dependence of the increase in cluster area on the cultivation times of ESE clusters of clones (2/32, E2, PE14) of the Norway spruce and clone PE 14 of blue spruce. At the beginning of the experiment, the average cluster area for each clone was 10 mm^2. Other experimental details are described in Fig. 5

The influence of lead on ESEs

Plant cells, callus, tissues and organs cultivated in vitro are good tools for studying the responses of plants to heavy metal stress because the cultivation conditions are stable and the metal ions are a component of the cultivation medium [45–49]. When adverse concentrations of a metal ion are found, the physiological, biochemical and molecular biological responses of cultivated structures can be studied.

When we found that IA was suitable for detecting the growth characteristics of ESE clusters, we then tested the influence of Pb-EDTA, which is known to be toxic to organisms [36], on the growth of ESE clusters of clone 2/32. We used lead chelate (Pb-EDTA) as the source of lead ions because the lead from salts such as nitrite, chloride or acetate partly precipitates with other components of the culture medium, making it difficult to determine the final concentration of lead ions [16]. We observed the growth of the individual ESE clusters in the presence of lead (0, 50, 250 and 500 μM of Pb-EDTA) (Fig. 8A). We did not examine the difference in the increase in ESE cluster area between the control and the lowest concentration of Pb-EDTA (50 μM) applied. Decreased growth occurred when a concentration of 250 μM Pb-EDTA was applied. Furthermore, we observed increased growth in area for ESE clusters treated with 500 μM Pb-EDTA in comparison with 250 μM Pb-EDTA (Fig. 8A). Besides growth, we studied the viability of treated ESEs by double staining (PI and FDA) (see

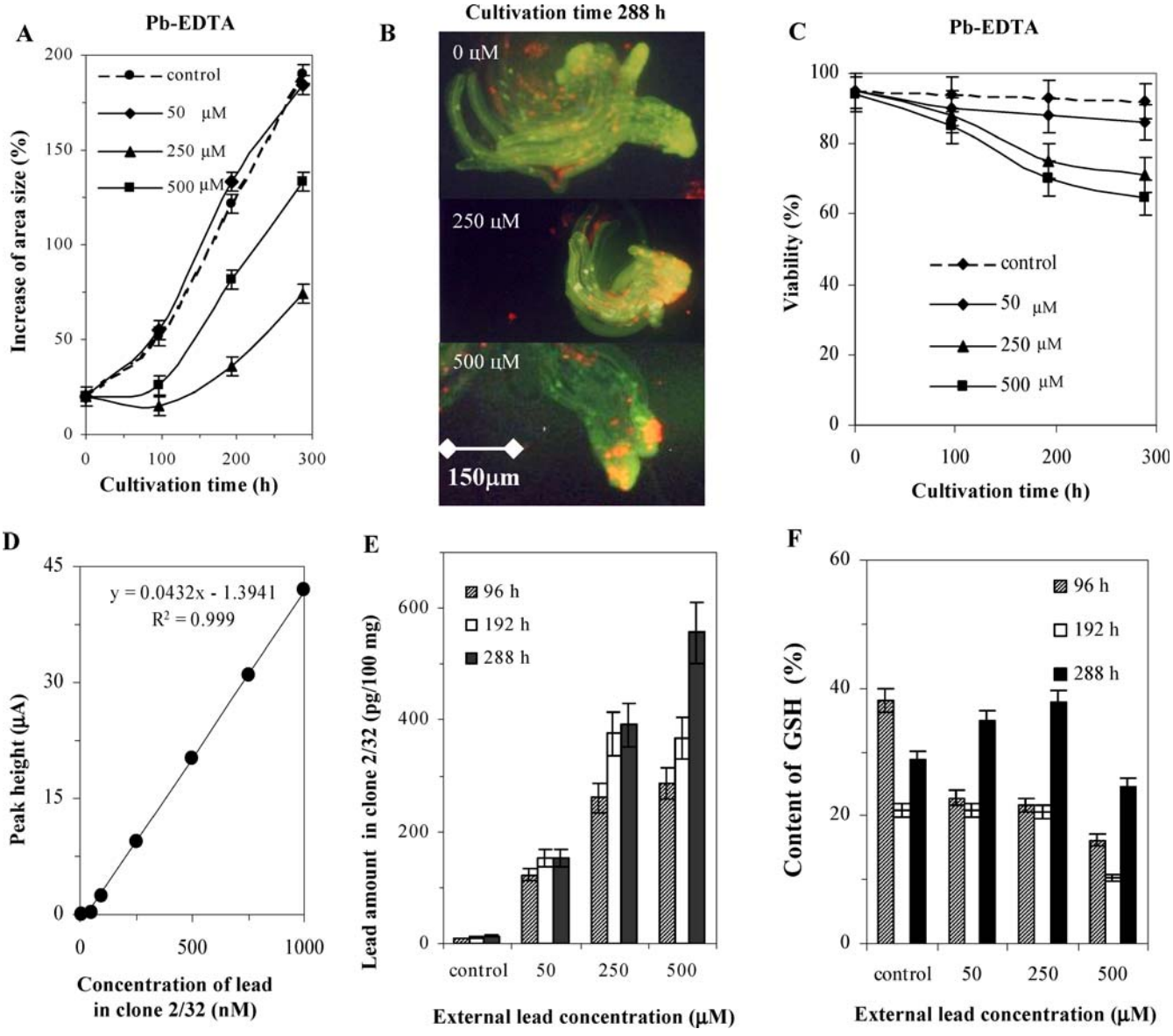

Fig. 8A–F The effect of Pb-EDTA (0, 50, 250 and 500 μM) on ESEs after 96,192 and 288 hours of cultivation. **A** Dependence of the growth in ESE cluster area. **B** Fluorescence microscope photograph of double staining after 288 h of cultivation at 0, 250 and 500 μM of Pb-EDTA. **C** Dependence of viability. **D** Calibration dependence of DPASV lead signal on its concentration in nontreated ESE extract. **E** Lead concentrations. **F** Glutathione content; these were recalculated on the number of viable cells. Other experimental details are described in Fig. 7

Fig. 8B). The viability of the ESEs decreased almost linearly with increasing Pb-EDTA concentration and cultivation time (Fig. 8C). Finally, the presence of Pb-EDTA markedly slowed the growth of ESE clusters (by more than 65% at 250 μM of Pb-EDTA, 288 h of cultivation) and decreased the viability of the ESEs (by more than 30% at 500 μM of Pb-EDTA, 288 h of cultivation).

The concentration of lead in the ESEs was determined as a function of increasing Pb-EDTA concentration during cultivation (96,192 and 288 h) by differential pulse anodic stripping voltammetry (DPASV). The calibration dependence of the DPASV lead signal on its concentration obtained in the presence of nontreated ESE extract is shown in Fig. 8D (y=0.04x–1.39, R^2=0.999). The amount of lead detected in the ESEs was very low (tens to hundreds of pg of Pb in 100 mg of fresh weight of ESE clusters) and this amount increased with increasing applied Pb-EDTA concentration and time of cultivation (Fig. 8E). This effect is probably related to cell detoxification mechanisms such as glutathione synthesis [11, 36, 50] and the ability of the cell to survive in the presence of Pb-EDTA, because lead in chelate form can easily penetrate through cell walls and membranes. That is why we studied the influence of lead on the glutathione (GSH) content. We determined the GSH in ESE samples using high-performance liquid chromatography coupled with mass spectrometry (HPLC–MS). We ascertained that the GSH content in ESEs decreases for the first 96 hours of cultivation as a function of applied Pb-EDTA concentration (Fig. 8F), which probably relates to the marked stress caused by the subcultivation process. After 96 h of cultivation, the growth in the sizes of the ESE clusters increased and the ESEs started to metabolise. The highest content of GSH was observed at an applied Pb-EDTA concentration of 250 mM up to 192 h, after which it markedly decreased. The same trend was observable after 288 h. The decreasing synthesis of GSH in the presence of the highest Pb-EDTA concentration is probably caused by damage to numerous mechanisms sustaining homeostasis and involving GSH due to the metabolism of the detoxification of lead.

Conclusion

We proved that image analysis could be used to determine basic parameters for studying the influence of abiotic and biotic stresses on early somatic embryos (ESEs). In addition, the obtained results correlated well with methods and techniques commonly used for these purposes.

Acknowledgement The authors wish to thank Drs. Jindra Zelinková and Stephen Hardy for reading the English version of the manuscript and to Jan Vacek for technical assistance. This work was supported by the grants: FRVS No. 2348/F4A, GACR No. 525/04P132 and IGA MZLU No. 250061/2005.

References

1. Mohr H, Schopfer P (1995) Plant physiology. Springer, Berlin Heidelberg New York
2. Hader D-P (1992) Image analysis in biology. CRC, London
3. Ibaraki Y, Kenji K (2001) Comput Electron Agric 30:193–203
4. Olofsdotter M (1993) Plant Cell Rep 12:216–219
5. Gagna CE, Winokur D, Larnbert WC (2004) Cell Biol Int 28: 755–764
6. Chi C–M, Vits H, Staba EJ, Cooke TJ, Hu W–S (1994) Biotechnol Bioenerg 44:368–378
7. Chi C–M, Zhang C, Steba EJ, Cooke TJ, Hu W–S (1996) Biotechnol Bioenerg 50:65–72
8. Hamalainen JJ, Kurten U, Kauppinen V (1993) Biotechnol Bioenerg 41:35–42
9. Padmanabhan K, Cantliffe DJ, Harrell RC, Harrison J (1998) Plant Cell Rep 17:681–684
10. Honda H, Ito T, Yamada J, Hanai T, Matsuoka M, Kobayashi T (1999) J Biosci Bioeng 87:700–702
11. Schroder P, Fischer C, Debus R, Wenzel A (2003) Environ Sci Pollut Res 10:225–234
12. Nagy J (1996) Novenytermeles 45:297–305
13. Nziguheba G, Merckx R, Palm CA, Mutuo P (2002) Agroforest Syst 55:165–174
14. Ward JMJ, Stromberg EL, Nowell DC, Nutter FW (1999) Plant Dis 83:884–895
15. Kizek R, Vacek J, Trnkova L, Klejdus B, Kuban V (2003) Chem Listy 97:1003–1006
16. Vacek J, Petrek J, Havel L, Klejdus B, Kizek R, Trnková L, Jelen F (2004) Bioelectrochemistry 63:347–351
17. Klejdus B, Zehnalek J, Adam V, Petrek J, Kizek R, Vacek J, Trnkova L, Rozik R, Havel L, Kuban V (2004) Anal Chim Acta 520:117–124
18. Grill D, Tausz M, Kok LJD (2001) Plant ecophysiology. Kluwer, Dordrecht
19. Cobbett CS (2000) Plant Physiol 123:825–832
20. Cobbett CS, Goldsbrough PB (2002) Annu Rev Plant Biol 53: 159–182
21. Noctor G, Gomez L, Vanacker H, Foyer CH (2002) J Exp Botany 53:1283–1304
22. Potesil D, Petrlova J, Adam V, Vacek J, Klejdus B, Zehnalek J, Trnkova L, Havel L, Kizek R (2005) J Chromatogr A 1084:134–144
23. Kizek R, Masarik M, Kramer KJ, Potesil D, Bailey M, Howard JA, Klejdus B, Mikelova R, Adam V, Trnkova L, Jelen F (2005) Anal Bioanal Chem 381:1167–1178
24. Masarik M, Kizek R, Kramer KJ, Billova S, Brazdova M, Vacek J, Bailey M, Jelen F, Howard JA (2003) Anal Chem 75: 2663–2669
25. Klejdus B, Mikelova R, Adam V, Zehnalek J, Vacek J, Kizek R, Kuban V (2004) Anal Chim Acta 517:1–11
26. Klejdus B, Vacek J, Adam V, Zehnalek J, Kizek R, Trnkova L, Kuban V (2004) J Chromatogr B 806:101–111
27. Klejdus B, Mikelova R, Petrlova J, Potesil D, Adam V, Stiborova M, Hodek P, Vacek J, Kizek R, Kuban V (2005) J Chromatogr A 1084:71–79
28. Klejdus B, Mikelova R, Petrlova J, Potesil D, Adam V, Stiborova M, Hodek P, Vacek J, Kizek R, Kuban V (2005) J Agric Food Chem 53:5848–5852
29. Vitecek J, Adam V, Petrek J, Babula P, Novotna P, Kizek R, Havel L (2005) Chem Listy 99:436–501
30. Vitecek J, Adam V, Petrek J, Vacek J, Kizek R, Havel L (2004) Plant Cell Tis Org 79:195–201
31. Tung G, Temple PJ (1996) Environ Tox Chem 15:906–914
32. Jokinen KJ, Durzan DJ (1994) Silva Fenn 28:95–106
33. Durzan DJ, Jokinen K, Guerra MP, Santerre A, Chalupa V, Havel L (1994) Int J Plant Sci 155:677–688

34. von Arnold SJ (1987) Plant Physiol 127:233–244
35. Havel L, Durzan DJ (1996) Int J Plant Sci 157:8–16
36. Vassil AD, Kapulnik Y, Raskin I, Salt DE (1998) Plant Physiol 117:447–453
37. Jones KH, Senft JA (1985) J Histochem Cytochem 33:77–79
38. Kizek R, Vacek J, Trnkova L, Jelen F (2004) Bioelectrochemistry 63:19–24
39. Bromba MUA, Ziegler H (1981) Anal Chem 53:1583–1586
40. Camera E, Rinaldi M, Briganti S, Picardo M, Fanali S (2001) J Chromatogr B 757:69–78
41. Nagmani R, Diner AM, Garton S, Zipf AE (1995) In: Jain SM, Gupta PK, Newton RJ (eds) Somatic embryogenesis in woody plants. Kluwer, Dordrecht, pp 23–48
42. Havel L, Durzan DJ (1999) In Jain SM, Gupta PK, Newton RJ (eds) Somatic embryogenesis in woody plants, Kluwer, Dordrecht, pp 125–147
43. Smith MAL, Spomer LA (1987) In Vitro Cell Dev Biol 23:67–74
44. Steward N, Martin R, Engasser JMk, Goergen JL (1999) Plant Cell Rep 19:171–176
45. Weber G, Konieczynski P (2003) Anal Bioanal Chem 375:1067–1073
46. Sanz–Medel A, Montes–Bayon M, Saanchez MLF (2003) Anal Bioanal Chem 377:236–247
47. Silva MM, Vale MGR, Damin ICF, Welz B, Mandaji M, Fett JP (2003) Anal Bioanal Chem 377:165–172
48. Zehnalek J, Hanustiak P, Petrek J, Potesil D, Adam V, Havel L, Babula P, Kizek R (2005) Listy Cukrov 120:142–145
49. Strouhal M, Kizek R, Vacek J, Trnkova L, Nemec M (2003) Bioelectrochemistry 60:29–36
50. Meagher RB (2000) Curr Opin Plant Biol 3:153–162